Available online at www.sciencedirect.com

ScienceDirect

Energy Procedia 158 (2019) 1249–1254

Energy Procedia

www.elsevier.com/locate/procedia

10th International Conference on Applied Energy (ICAE2018), 22-25 August 2018, Hong Kong, China

Performance Study on an Unglazed Photovoltaic Thermal Collector Running in Sichuan Basin

Ying Yu[a,b], Enshen Long[b], Xi Chen[a], Hongxing Yang[a,*]

[a]*Renewable Energy Research Group (RERG), Department of Building Services Engineering, The Hong Kong Polytechnic University, Hong Kong, China*
[b]*College of Architecture and Environment, Sichun University, Chengdu 610065, China*

Abstract

A performance study with experiments and TRNSYS simulations was conducted for a roll-bond water-type photovoltaic thermal (PVT) collector installed in Chengdu, Sichuan Basin. The measured ambient data and operation data were input to two TRNSYS models and their results were compared. The two numerical models have their own advantages in the simulation of thermal and electrical properties of the PVT collector. By calibrating the models with experimental data, the deviation between the simulated and the measured values was further reduced. In addition, the excellent performance of the roll-bond PVT absorber was also validated by the steady-state test results. However, the long-term system performance is subject to further investigations.

Keywords: Roll-bond absorber; Thermal efficiency; PV efficiency; Pressure drop; TRNSYS

1. Introduction

A photovoltaic thermal (PVT) module can produce electricity as well as heat simultaneously. The typical absorber of a flat-plate PVT collector is the sheet-and-tube plate, while the roll-bond and fully-wetted types are its variants. For these three types of thermal absorber, Aste et al. [1] listed their main features and different manufacturing techniques. The roll-bond absorber was already used in solar collectors [2] and had shown good

* Corresponding author. Tel.: +00852-2766 5863; fax: +00852-2774 6146.
E-mail address: hong-xing.yang@polyu.edu.hk

10.1016/j.egypro.2019.01.414

performance. Recently, they have been frequently applied to hybrid PVT collectors. The channel configurations of them include harp (parallel), serpentine arrangements, like those of common sheet-and-tube absorbers, and a variety of bionic configurations.

Both electrical and thermal power output predictions for a PVT collector are important tasks in design and planning. Florschuetz's PVT collector model was adapted from the steady-state model of flat-plate collector [3]. Lately, Zondag et al. [4] built four numerical models to study the thermal performance of a PVT collector, applying to 9 different PVT designs [5]. Chow [6] developed a dynamic model to analyze the transient performance of a glazed sheet-and-tube PVT water collector. On the other hand, experimental research for comparing different PVT types [7] and for validating model performances had been carried out [8]. As a simulation tool for renewable energy system, TRNSYS had been used to model and simulate PVT systems [9, 10]. The numerical models of PVT in TRNSYS were for traditional sheet-and-tube absorber based on Florschuetz's PVT model and suitable for predicting the performance of the PVT integrated with parallel-channel absorber. However, for roll-bond PVT collectors, the channels were not circular and mostly non-parallel. So far, few studies have been done to examine the software's applicability to roll-bond PVT.

This paper presents the experimental and simulation work on an unglazed PVT system with poly-crystalline silicon solar cells and a roll-bond absorber plate characterized by harp channel arrangement. It forms the fundamental work of a project for PVT application which was designed for the rural family for domestic hot water (DHW) and partial electricity supply. This work was related to further simulation of non-parallel-channel absorbers.

Nomenclature

A_c	area of the collector, normally gross area, m^2	T_a	ambient temperature, ℃
C_p	specific heat capacity of water, kJ/kg·℃	T_{fi}	inlet fluid temperature, ℃
F'	PVT collector efficiency factor	T_{fo}	outlet fluid temperature, ℃
F_R	PVT collector heat removal factor	T_{fm}	mean fluid temperature, ℃
G_T	global solar irradiance on the module plane, W/m^2	η_e	electrical efficiency
$\dot{m}$	flow rate of fluid through the PVT collector, kg/s	η_{th}	thermal efficiency
Q_u	useful heat gain of fluid, W	$(\tau\alpha)_{\text{eff}}$	effective transmittance-absorptance product
S	effective absorbed solar radiation for absorber plate, W/m^2		
β_r	temperature coefficient of solar cell efficiency, %/℃	**Subscript**	
β_G	incident radiation coefficient of solar cell efficiency, % m^2/W	*ref*	refers to the reference conditions
U_L	overall heat loss coefficient from the absorber to the ambient, W/m^2·K		(i.e. G_T=1000W/m^2, T_{PV}=25℃, AM=1.5)

2. System description

The PVT test rig consisted of a PVT module, a water tank, as well as some control valves and check valves, connected with polypropylene random (PP-R) pipe as an open natural-circulation loop system, meanwhile, a stand-by pump was connected in parallel as the bypass of the loop and worked as needed. Figure 1 shows the schematic diagram of the test rig. The PV module adopted was a semi-finished commercial product of size 1480×670×5mm, comprised of 36 poly-crystalline (mc-Si) solar cells. The thermal absorber was a roll-bond aluminium plate of 1450×640×1.5mm. In order to decrease water loop resistance, especially the pressure drop in absorber, the parallel channel, so called harp configuration was chosen. The specifications and design parameters of the components are shown in Table 1. The hybrid collector was insulated by 40mm rubber plastic foam at the back side of the absorber plate. Its thermal conductivity is 0.036 W/m·K.

Table 1. Specifications of PV lamination and parameters of thermal absorber.

Parameter	Value
Maximum power (STC)	153.04Wp
Maximum voltage	18.03V

Maximum current	8.80A
Open circuit voltage	22.45V
Short circuit current	9.34A
Temperature coefficient of solar cell efficiency	-0.44%/℃
Number of channels in the absorber	18
channel distance	80mm
channel length	600mm
Cross section area of a channel	19.7mm^2
Hydraulic diameter of the channel (non-circular)	3.25mm

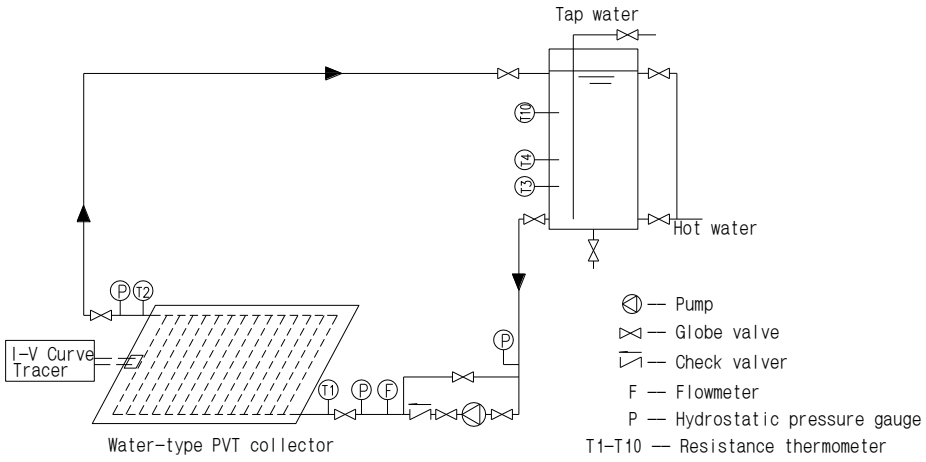

Fig. 1. Schematic diagram of the PVT test rig

3. Methods

3.1. Experiments

When the PVT test rig was installed on the roof of a residential building in Chengdu, the daily performance monitoring was carried out under the typical local weather condition. The measure devices included flowrate sensors, resistance temperature detectors, an I-V Curve Tracer and Pyranometers. Apart from the I-V curve measured with 2-minite test cycle, all other data were recorded at 1-minute intervals by data acquisition devices.

For thermal performance tests, there are steady-state and quasi-dynamic test conditions according to American [11] and European standards [12]. Based on the measurement of water temperatures at the inlet and outlet of the PVT collector, T_{fi} and T_{fo}, the flow rate $\dot{m}$, and the incidence solar irradiance, G_{T}, as well as V_{mpp} and I_{mpp}, the checked voltage and electric current at the maximum power point operation, the thermal and electrical performance of the test module can be given by:

$$\eta_{th} = \frac{\dot{m}C_p\left(T_{fo} - T_{fi}\right)}{G_T A_c} \tag{1}$$

$$\eta_e = \frac{V_{mpp} I_{mpp}}{G_T A_c} \tag{2}$$

3.2. Simulation

The analytical approach was based on the energy balance equation of the PVT module. The thermal output of the PVT is decided by its operating condition and some attribution parameters such as the overall heat loss coefficient U_L, the collector efficiency factor F' or the heat removal factor F_R. The useful heat gain of the PVT collector is：

$$Q_u = A_c F_R\left[S - U_L\left(T_{fi} - T_a\right)\right] = A_c F'\left[G_T(\tau\alpha)_{\text{eff}}(1-\eta_e) - U_L\left(T_{fm} - T_a\right)\right] \quad (3)$$

$$\eta_{th} = \frac{Q_u}{G_T A_c} \quad (4)$$

In this work, the designated PVT system was constructed in TRNSYS Simulation Studio with Type50a and Type560 respectively. Because of its non-circular channel, the hydraulic diameter was adopted instead of diameter parameter. The thermal network of Type50a was simplified on the basis of the approximation that the cell temperature was equal to the absorber temperature. In addition, Type50a took the U_L, $(\tau\alpha)_{\text{eff}}$, and F' as constants. By contrast, Type560 was more complicated. It defined the overall heat loss coefficient U_L as the function of the ambient temperature T_a, wind speed V and angle of incidence θ.

The factors that affected the actual PV efficiency include temperature of solar cells, angle of incidence, solar spectrum, and low irradiance. Mostly, the temperature factor was only taken into account. The electrical output of the PVT collector was assumed to vary linearly with the cell temperature. Based on parameters under Standard Test Conditions and temperature coefficient of cells β_r, the real PV efficiency is given by:

$$\eta_e = \eta_{\text{ref}}[1 - \beta_r(T - T_{\text{ref}})] \quad (5)$$

Besides temperature factor, Type560 model related PV efficiency linearly to the incident radiation.

4. Results and discussion

4.1. Pressure drop

The resistance of the water loop determines the water circulation mode in the PVT collector. To find the possibility of natural-circulation in this PVT collector, pressure drops of the roll-bond absorber at different flowrates were measured. They are the main share of the water resistance in the loop. It was found that the pressure drop was close to linear growth from 100Pa (at 0.1L/min·m^2) to 400Pa (at 2.0L/min·m^2), as shown in Fig. 2.

In the earliest test, when the water tank was set above the PVT collector of 1.2 metre, the natural circulation was observed with a very small flow rate under 0.2L/min·m^2, and a notable temperature difference above 20℃, which was detrimental to conversion efficiency of PV cells. According to the pressure drop feature of the PVT collector, if the central-point height difference between the water tank and the PVT panel increased to 4m, the flowrate of 0.8 L/min·m^2 would be obtained by gravity circulation with a water temperature difference about 10℃. The case is applicable to low-rise housing in rural areas with abundant space in front of house. Otherwise, the mechanical circulation has to be adopted without such conditions.

4.2. Thermal and electrical efficiency

The tests were operated in Chengdu for several days every month from June, 2017 to May, 2018. According to thermal performance test standards for steady-state conditions, the inlet water temperatures were controlled within 30-45℃, with the flow rate between 1.0-1.41L/min·m^2, adjusted by control valves of the circulation pump. The ambient temperature was under 30℃. The annual wind speed in Sichuan Basin is very low, mostly ranged from 0-2m/s.

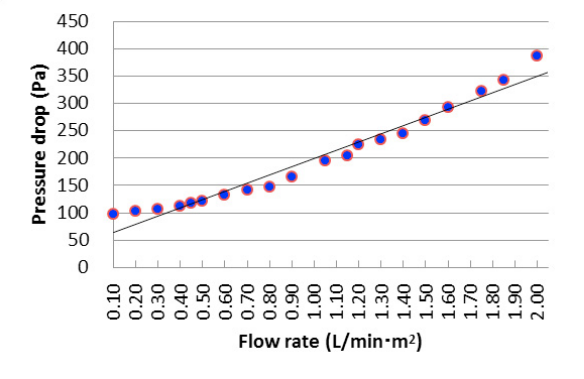

Fig. 2. Pressure drop of the PVT absorber plate

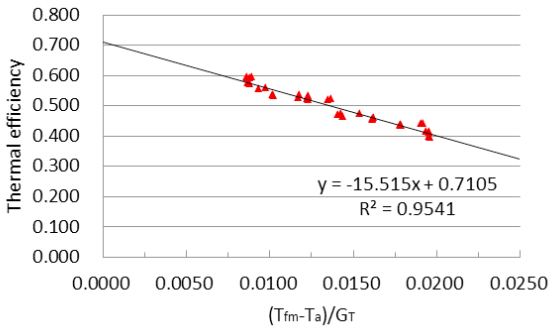

Fig. 3. Thermal efficiency of the PVT collectors

Fig. 3 shows the transient thermal efficiencies of the test on April 16th, 2018 around solar noon with solar radiation more than 800W/m^2. The ambient temperature was 24.5±1.5℃ and wind speed varied between 2.0-4.0m/s. The flow rate of the absorber plate was 1.24L/min·m^2. The test data were plotted as η_{th} versus $(T_{fm}- T_a)/G_T$, the reduced temperature, and T_{fm} is the arithmetic average of inlet and outlet water temperatures.

The thermal efficiency is conventionally expressed as a function of the reduced temperature, and the equation (4) can be given in a linear expression:

$$\eta_{th} = F'\left[(\tau\alpha)_{eff}(1-\eta_e) - U_L\frac{(T_{fm}-T_a)}{G_T}\right] = \eta_{t0} - a_1\frac{(T_{fm}-T_a)}{G_T} \quad (7)$$

where η_{t0} is the thermal efficiency at zero reduced temperature, a_1 relates to the PVT collector heat loss coefficient. From Fig. 3, the thermal efficiency at zero reduced temperature is 0.71, occurred when the average water temperature equals to the ambient temperature. And a_1 is 15.515W/m^2·K, well matched with the theoretical calculation values of average U_L (16.88 W/m^2·K) and F' (0.92) for this hybrid collector.

There had been a certain decline in both thermal and electrical performance of the PVT collector by the end of the experimental period, especially for electrical performance. Before 2018, the electrical efficiency was recorded among 11.0% - 15.0%, and the reference efficiency of PV module was 15.4% (STC). However, data records from the performance test from the March of 2018 showed the PV efficiencies fluctuating between 10.3% - 13.0%.

4.3. Simulation results

By inputting the measured ambient data and operation data of the PVT to TRNSYS, the simulated useful heat gain Q_u and output power Q_e were obtianed, and then compared with calculated measured values respectively. The difference between the simulated values from the measured values was represented by the root mean square deviation (RMSD). For useful heat gain Q_u, the RMSDs of 68.7 W/m^2 and 60.2 W/m^2 were obtained by Type50a and Type560 respectively. While for electric power Q_e, the RMSDs of 7.4 W/m^2 and 11.2 W/m^2 were acquired by Type50a and Type560 respectively. In most test points, shown in Fig. 4 and Fig. 5, both models produced the smaller simulated Q_u than the measured Q_u, but had the larger simulated Q_e than measured Q_e, which probably caused by the overestimated the overall heat loss U_L. By reducing the convective loss of the PVT panel, both calibrated models achieved lower deviations from the measured values, presented by RMSDs in Q_u of 46.9 W/m^2 and 35.1 W/m^2 for Type50a and Type560 respectively and in Q_e of 5.8 W/m^2 and 9.7 W/m^2 respectively.

The simulated PV efficiencies almost remained stable, different from the measured, fluctuant values, especially during one hour close to sunrise and sunset, because the effects of solar spectrum and low irradiance had not been taken into accounted.

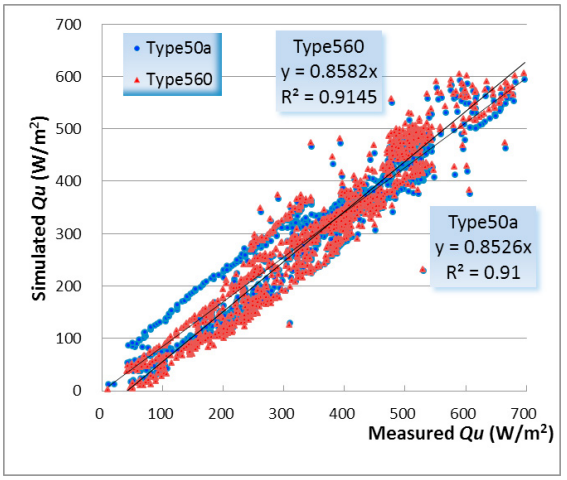

Fig. 4. Comparison of simulated and measured *Qu*

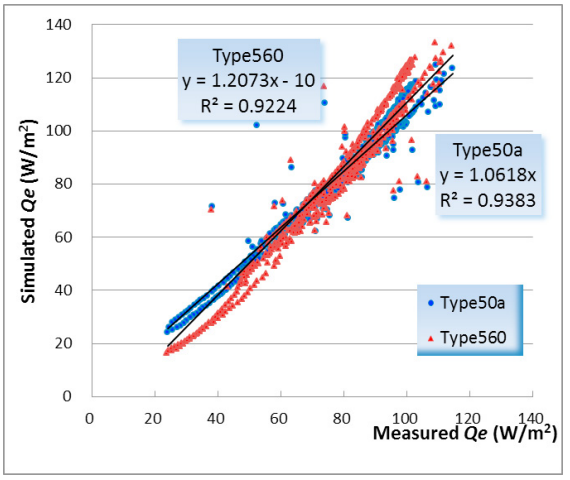

Fig. 5. Comparison of simulated and measured *Qe*

5. Conclusion

The paper presents the experimental and simulation study on a low-cost roll-bond PVT collector. The results showed that: 1. the PVT system has a low water resistance in the loop, but mechanical circulation is still needed for obtaining the suitable flow rate to achieve better performance; 2. the thermal efficiency of the PVT collector at zero reduced temperature was about 71%, indicating the good thermal performance of the roll-bond absorber; 3. the complicated model Type560 tended to simulate accurately in thermal performance while the simple Type50a could have better prediction of electrical output. When considering simulation cost of the two models, Type50a is slightly superior to Type560 and worth adopting.

Acknowledgements

The author would like to express appreciation to the department of building services engineering, the Hong Kong Polytechnic University for providing testing devices and software support for this study.

References

[1] Aste N, del Pero C, Leonforte F. Water flat plate PV–thermal collectors: A review. Solar Energy. 2014;102:98-115.
[2] Hermann M. Develop of a Bionic solar collector with alluminium roll-bond absorber. 2011.
[3] Florschuetz L. Extension of the Hottel-Whillier model to the analysis of combined photovoltaic/thermal flat plate collectors. Solar energy. 1979;22:361-6.
[4] Zondag HA, de Vries DW, van Helden WGJ, van Zolingen RJC, van Steenhoven AA. The thermal and electrical yield of a PV-thermal collector. Solar Energy. 2002;72:113-28.
[5] Zondag HA, de Vries DW, van Helden WGJ, van Zolingen RJC, van Steenhoven AA. The yield of different combined PV-thermal collector designs. Solar Energy. 2003;74:253-69.
[6] Chow TT. Performance analysis of photovoltaic-thermal collector by explicit dynamic model. Solar Energy. 2003;75:143-52.
[7] Kim J-H, Kim J-T. The experimental performance of an unglazed PVT collector with two different absorber types. International Journal of Photoenergy. 2012;2012.
[8] Del Col D, Padovan A, Bortolato M, Dai Prè M, Zambolin E. Thermal performance of flat plate solar collectors with sheet-and-tube and roll-bond absorbers. Energy. 2013;58:258-69.
[9] Haurant P, Ménézo C, Gaillard L, Dupeyrat P. A Numerical Model of a Solar Domestic Hot Water System Integrating Hybrid Photovoltaic/Thermal Collectors. Energy Procedia. 2015;78:1991-7.
[10] Nualboonrueng T, Tuenpusa P, Ueda Y, Akisawa A. The performance of PV –t systems for residential application in Bangkok. Progress in Photovoltaics: Research and Applications. 2012;21:1204-13.
[11] ASHRAE. ANSI/ASHRAE Standard 93-2010 (RA 2014) Methods of testing to determine the thermal performance of solar collectors. 2014.
[12] EuropeanStandard. EN 12975-2:2006 Thermal solar systems and components-Solar collectors-. Part 2: Test methods2006.